

Spatial-Temporal Variations and Trends in Freezing Level Height in Iran: An Analytical Perspective

Hasan Ghadermazi ^a, Jafar Masoompour Samakosh^{b*}, Seyed Ehsan Fatemi ^c, Maryam Hafezparast^d

^aPh.D Candidate in Climatology, Department of Geography, Faculty of Literature and Humanities, Razi University, Kermanshah, Iran. (hasan.ghadermazi@gmail.com)

^{b*}Associate Professor, Department of Geography, Faculty of Literature and Humanities, Razi University, Kermanshah, Iran. (j.masoompour@razi.ac.ir)

^cAssociate Professor, Department of Water Engineering, Campus of Agriculture and Natural Resources, Razi University, Kermanshah, Iran. (se.fatemi92@gmail.com)

^dAssistant Professor, Department of Water Engineering, Campus of Agriculture and Natural Resources, Razi University, Kermanshah, Iran. (maryam.hafezparast2@gmail.com)

Abstract

This research has been performed to investigate the temporal and spatial changes of freezing level height in Iran in the statistical period from 1940 to 2023 using the modified Mann-Kendall non-parametric analysis method. The results of the study show that the freezing level height shows a significant upward trend from December to April. Except summer, the upward trend of seasonal changes in the freezing level height is quite evident in autumn, winter, and spring. The annual changes in the freezing level height show a significant upward trend during the period. Significant upward trends on a monthly, seasonal, and annual scale can show one of the consequences of climate change in Iran. The results of the survey of spatial changes show that the height of the freezing level has an inverse relationship with the latitude, and as the latitude decreases (towards southern regions of Iran), the height of the freezing level increases. This relationship is more in winter. The correlation coefficient of FLH changes with latitude is significant at the alpha level 0.05. The relationship between the changes in the height of the freezing level and the longitude is direct. As we move towards the east, the height of the freezing level also increases. The highest level of freezing level height is observed in Chabahar (4347.5 meters) in southeastern Iran. **Considering the decrease in snow cover and increase in heavy rainfall in Iran, assessing variations in freezing level height can be useful for predicting these variables.**

Key Word: Freezing Level Height, Trend, Sen's slop, Iran

1. Introduction

The freezing level height (FLH) is the height of the location where the air temperature is 0°C (isotherm), and indicates the approximate location of the phase transition of water between solid and liquid and sublimation from solid to vapor. FLH is a critical parameter of hydrological conditions and climate change (Guo et al., 2021).

At levels above the freezing height, the air temperature is below zero degrees and at lower levels, the temperature is above zero degrees. The height of the freezing level or the isothermal line of zero degrees in the atmosphere is a parameter that determines the ice cover of mountains and high areas with the change of water to ice (Harris et al., 2000; Vuille et al., 2004; Coudrain et al., 2005; Vuille et al., 2008).

The height of the freezing level in high mountain areas is an essential parameter in the durability and extent of the snow and freezing cover, and plays a prominent role in melting and freezing. This parameter also affects the amount and status of water resources (Diaz and Graham, 1996; Harris et al., 2000; Diaz et al., 2003; Bradley et al., 2009; Folkins, 2013).

Unfortunately, climate and hydrological research in the cryosphere faces limitations due to the lack of sufficient climate data from icy and high mountain areas. Considering the mentioned obstacles, the FLH survey obtained from radiosonde data or network data can provide more accurate information to detect changes in the cryosphere,

the extent of snow cover, and its response to climate change. In addition, with low FLH in the atmosphere and strong updrafts, hail formation is enhanced (Dessens, 1986). **On the other hand, data limitations prevent a detailed examination of seasonal and monthly trends (Khansalari, 2020).**

The results of previous research show that the height of the freezing level has been increasing since the late 1950s on a global scale in tropical regions and especially in the extratropical regions. This increase in temperature has had a significant impact on the conditions of the cryosphere and snowy mountain areas (Diaz and Graham, 1996; Gaffen et al., 2000; Harris et al., 2000; Diaz et al., 2003; Seidel and Free, 2003; Bradley et al., 2009). The rate of temperature increase has caused FLH to increase with increasing altitude. This phenomenon is significantly more severe in mountainous regions (Diaz et al., 2014; Pepin et al., 2015). Recent studies in China clearly show, on a regional scale, the warming of land surface temperature and tropospheric air temperature and the increase of FLH since the 1960s (Zhang and Guo, 2011; Chen et al., 2012; Dong et al., 2012; Huang et al., 2013; Wang et al., 2014; Zhang et al., 2014a; Zhang et al., 2014b).

Since the freezing level height is closely related to rain and snow depth, it is important to study its changes and how it is associated with the type of precipitation and cold waves and frost, especially in mountainous areas. It is also an essential parameter for changes in the cryosphere, because it indicates the approximate location of permanent ice and snow on the Earth's surface. Therefore, the freezing level is an important indicator of climate variability and change. Considering these cases, it becomes necessary to conduct comprehensive and more detailed studies of the freezing level height in Iran, which has different climatic regions and complex topography, which is also important in determining the status of water resources.

2. Methods

2.1. The study area

Iran is one of the vast countries in the world, located in the range of 25°3' to 39°47' north latitude and 44°5' to 63°18' east longitude and in the Middle East region as well as the vicinity of Central Asia and the Caucasus (Figure 1). Due to its geographical location, which has changes in altitude, distance from the sea, wideness and long distance between north and south, which covers from latitude 25 degrees to 40 degrees north, it has a very diverse climate. Therefore, the humidity conditions in this land vary from very dry to very humid. The amount of rainfall fluctuates in different regions of the country and varies significantly from year to year.

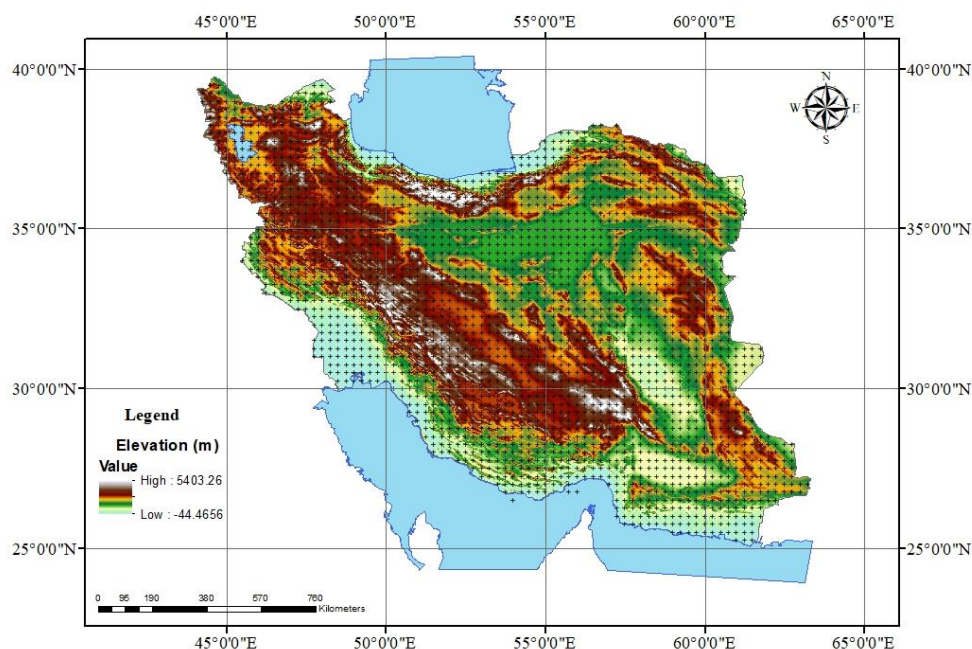


Figure 1- Geographical location of Iran and spatial distribution of network data, 0.25 * 0.25

2.2. Data

In this research, the average raster data of the freezing level with a resolution of 0.25 x 0.25 in 12 hours of every month during the years 1940 to 2023 have been used. The mentioned data was downloaded from the Climatic database of the European Centre for Medium-Range Weather Forecasts (ECMWF). The selected range includes from 44 Degrees east longitude to 64 Degrees east longitude and from 23 Degrees north latitude to 44 Degrees north latitude (location of Iran). For statistical analysis, network data were converted into vector data in GIS software, and level maps of freezing level were extracted. The statistical parameters of the monthly freezing level from 1940 to 2023 are shown in Table 1. According to Table 1, the average FLH is at the lowest altitude (1347 m) in January and the highest altitude (4145.8 m) in July.

2.3. Methods

Monthly maps of freezing level elevation (1009 months) were extracted for trend analysis. Then, the maps of the same months were arranged as time series for each twelve months, and the trend of changes in the time series for each month was analyzed using the modified nonparametric Mann-Kendall test.

One of the conventional methods in the analysis of climate data time series is to examine the presence or absence of trends in them caused by gradual natural changes and climate changes caused by human activities (Liu et al., 2020).

The nonparametric Mann-Kendall test, as a suitable method for proving the existence of trends in climate series, has been used in recent years as the best option for examining the existence of seasonal and annual changes in climate variables such as temperature and precipitation (Lornezhad et al., 2023). The Mann-Kendall method was first proposed by Mann (1945) and then extended and developed by Kendall (1970). The zero hypothesis of the Mann-Kendall test indicates the randomness and absence of a trend in the data series, and accepting the one hypothesis (rejection of the null hypothesis) suggests the presence of the trend in the data series (Sen, 1968).

2.3.1. Mann-Kendall Test (MK)

The Mann—Kendall (MK) analysis uses non-parametric trend development only for reliable data. It has been generally practical where the data are not identical to a normal distribution (non-parametric). The Mann-Kendall test is used globally to analyze trends in meteorological variables (Tabari et al., 2015). World Metrological Data has been widely suggested for this test for free use by the public to assess trends (Shi et al., 2013) and to detect the statistically significant trends of long-term data. Two hypothesis tests must be tested in the MK, Null hypothesis and, Alternative Hypothesis. The null hypothesis defines the absence of a trend in the time series of data, while the alternative hypothesis states that there is a significant trend in the time series. The MK test does not require the assumption of normality, and not only indicates the direction but also the magnitude of significant trends. The Mann-Kendall test measured values ($X_j - X_k$), where $j > k$ and test statistics S is computed exerting the formula.

$$S = \sum_{k=1}^{n-1} \sum_{j=k+1}^n \text{sign}(x_j - x_k) \quad (1)$$

Where X_j and X_k are the annual values in years j and k , $j > k$, respectively.

$$\text{sign}(x_j - x_k) \begin{cases} 1 & \text{if } (x_j - x_k) > 0 \\ 0 & \text{if } (x_j - x_k) = 0 \\ -1 & \text{if } (x_j - x_k) < 0 \end{cases} \quad (2)$$

It is necessary to compute the probability associated with S and the sample size n, to quantify the significance of the trend statistically, The calculating formula of variance S is denominating as;

$$Var(S) = \frac{[n(n-1)(2n+5) - \sum_{p=1}^q t_p(t_p-1)(2t_p+5)]}{18} \quad (3)$$

Where q is defined as the number of tied groups and t_p is the number of data in the pth group. The values of S and VAR(S) are accustomed to calculate the test statistics Z, which is following as;

$$Z = \begin{cases} \frac{s-1}{\sqrt{Var(s)}} & \text{if } S > 0 \\ 0 & \text{if } S = 0 \\ \frac{s+1}{\sqrt{Var(s)}} & \text{if } S < 0 \end{cases} \quad (4)$$

Z score follows a normal distribution. At a Level of $\alpha=0.05$ (95% confidence interval) and two-sided alternative, the critical values of 0.025 are equal to -1.96 to 1.96. The trend is said to be decreasing if Z is negative and the absolute value is greater than the level of significance, while it is increasing if Z is positive and greater than the label of significance. If $n \leq 10$ the normal approximation test is used and a statistically significant trend is computed exerting the Z score. Mann Kendall & Sen's slope estimator test the Z score significance level at $\alpha: 0.001, 0.05,$ and 0.1.

The test statistics τ can be computed as;

$$\tau = \frac{s}{n - (n-1)/2} \quad (5)$$

2.3.2. Mann-Kendall test with trend-free pre-whitening (TFPW)

When the autocorrelation is positive or negative, there will be a decrease or increase in the value of S, which will be under- or overestimated by the original variance V(S) (Hamed, 2009). Therefore, when trend analysis is conducted for this data using MK1, it will show positive or negative trends when there is no trend. Hence, the trend free pre-whiting process (TFPW) was proposed (Hamed, 2009), which the slope and lag-1 serial correlation coefficient are simultaneously estimated. The lag-1 serial correlation coefficient is then corrected for bias before pre-whitening. Finally, the lag-1 serial correlation components are removed from the series before applying the trend test. The following steps are used to determine trend analysis using the MK2 test. Calculate the lag-1 ($k = 1$) autocorrelation coefficient (r_1) using:

1-Calculate the lag-1 ($k = 1$) autocorrelation coefficient (r_1) by:

$$r_1 = \frac{\frac{1}{n-k} \sum_{i=1}^{n-k} (x_i - \bar{x})(x_{i+k} - \bar{x})}{\frac{1}{n} \sum_{i=1}^n (x_i - \bar{x})^2} \quad (6)$$

If $\frac{-1-1.96\sqrt{n-2}}{n-1} \leq r_1 \leq \frac{-1+1.96\sqrt{n-2}}{n-1}$ is satisfied, then the series is assumed to be independent at a 5% significance level and there is no need for pre-whitening.

Otherwise, pre-whitening is required for the series before applying the MK1 test.

Equation (7) is used to remove the trend in time series

$$X'_i = X_i - (\beta \times i) \quad (7)$$

Data to get a detrended time series.

Where

$$\beta = \text{Median} = \left[\frac{x_j - x_i}{j - i} \right] (\forall j > i) \quad (8)$$

Using Eq. (9), remove the lag-1 autoregressive component (AR (1)) from the detrended series to get a residual series as follow;

$$Y'_i = X'_i - r_1 * X'_{i-1} \quad (9)$$

Thus, the MK test is applied to the blended series Y_i to determine the significance of the trend.

2.3.4. Modified Mann-Kendall test with variance correction (MMK)

Sometimes, removing lag-1 autocorrelation is not enough for many Hydroclimatologic time series datasets. A correction procedure was proposed by (Hamed and Rao 1998) to overcome the limitation of serial autocorrelation in time series. First, the corrected variance S is calculated by Eq.(10), where $V(S)$ is the variance of the MK1, and CF is the correction factor due to the existence of serial correlation in the data. Corrected variance:

$$S(V \times (s)) = CF \times V(S) \quad (10)$$

Where

$$CF = 1 + \frac{2}{n(n-1)(n-2)} \sum_{k=1}^{n-1} (n-k)(n-k-1)(n-k-2)r_k^R \quad (11)$$

Where r_k^R is lag-ranked serial correlation, while n is the total number of observations. The advantage of the MK3 test over the MK2 test is that it includes all possible serial correlations (lag- k) in the time series, At the same time MK2 only considers the lag-1 serial correlation (Yue et al. 2002).

2.3.5. Sen's Slope Estimator

Sen (1986) presented a non-parametric method for time series analysis by developing and expanding a series of statistical studies conducted by Thiel (1950). This method, like the Mann-Kendall method, uses the difference analysis between the observations of a time series. Also, this test can be easily used when there are missing data. This method is based on calculating a median slope for the time series and judging the significance of the obtained slope at different confidence levels (Khorshiddoust et al., 2018). In this case of linear model $f(t)$ can be denominated as;

$$f(t) = Q_t + B \quad (12)$$

Where Q is the slope, B is constant. According to Pohlert (2020), initially, a set of linear slopes is calculated as follows (Eq. 13):

$$Q_i = \frac{x_j - x_k}{j - k} . i = 1.2.3. \dots N . j > k \quad (13)$$

If there are n values X_j in the time series, there will be as many as $N=n(n-1)/2$ slope estimate Q_i .

3. Results and discussion

The results of the monthly analysis of freezing level height in Iran show that the fluctuations of the freezing level are different during the months of the year (Table1). The height of the freezing level from December to March fluctuates from the ground level (zero level) to the height of 5894.1m during August. The highest fluctuation of freezing level height is observed in November (4966.5 m) and the lowest fluctuation is observed during July (3654.5 m). Monthly changes in freezing level elevation and data distribution relative to the mean for each month are shown (Figure 2).

Table1. Statistical parameters of the monthly FLH-(1940-2023)

Monthly	Absolute Max	Average	Absolute Min	Range	Sd	CV%
Jan	4347.5	1347.0	0.0	4347.5	173.4	12.9
Feb	4562.4	1486.0	0.0	4562.4	189.3	12.7
Mar	4654.1	1902.9	0.0	4654.1	196.4	10.3
Apr	5138.1	2537.0	226.5	4911.6	201.4	7.9
May	5458.8	3149.0	660.9	4797.9	166.4	5.3
Jun	5679.0	3790.9	1379.0	4300.0	149.0	3.9
Jul	5637.9	4145.8	1983.4	3654.5	147.6	3.6
Aug	5894.1	4017.4	1858.2	4035.9	147.9	3.7
Sep	5583.1	3610.8	1449.6	4133.5	148.3	4.1
Oct	5435.4	2935.8	40.2	5395.2	234.7	8.0
Nov	4997.9	2221.1	31.4	4966.5	211.4	9.5
Dec	4823.3	1666.2	0.0	4823.3	217.3	13.0
Season's average	Max	Average	Min	Range	Sd	%CV
Winter	2033.1	1576.7	1168.5	864.6	182.1	11.5
Spring	3420.6	3159.0	2858.9	561.6	122.8	3.9
Summer	4138.0	3924.7	3728.1	409.9	95.3	2.4
Autumn	2790.6	2274.3	1740.6	1049.9	158.2	7.0
Annual's average	Max	Average	Min	Range	Sd	%CV
(1940-2023)	3095.6	2733.7	2374	721.6	139.6	6.3

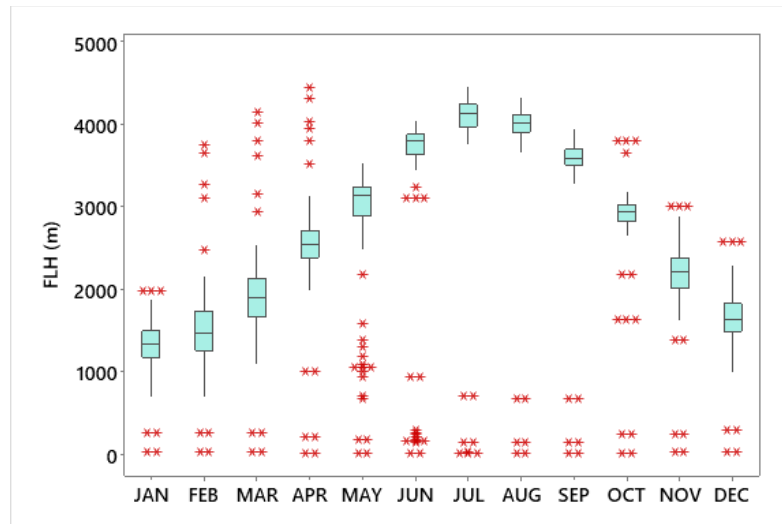


Figure 2. Boxplot of Monthly FLH (1940-2023)

3.1. Monthly trend analysis

Analysis of monthly freezing surface height trends based on the modified Mann-Kendall method is depicted in Figure 3. The monthly trend analysis results show that the freezing level's height from December to April shows a significant upward trend at the alpha level of 0.05. The trend of increasing the height of the freezing level during March and April is more intense and is significant at the alpha level of 0.01. In the summer season, there is an increase in the height of the freezing level based on the age gradient, but it is not statistically significant. (The noteworthy point is the substantial increase in the height of the freezing level in June). The results obtained from this study are consistent with the results of recent studies in China (YanJun Guo et al., 2021), the Andes Mountains (Mardens, 2020), and the Tibetan Plateau (Wang et al., 2014). It seems that the upward trend in increasing the height of the freezing level is in line with climate changes and global warming and shows the consequences of climate change in the region. The results of the analysis of the monthly trend of the freezing level are shown in Table 2. In Figures 3 and 4, the trend graphs of the monthly FLH and the trend slope are drawn based on the Mann-Kendall and Sen's method.

Table 2. Monthly Mann-Kendall Trend and Sen's slope of FLH (1940-2023)

Months	Kendall's tau	p-value	Sen's slope
Jan	0.147	0.011*	2.109
Feb	0.173	0.02*	2.852
Mar	0.232	0.009**	3.454
Apr	0.305	0<0001**	3.465
May	0.102	0.195	0.887
Jun	0.15	0.017*	1.037
Jul	-0.004	0.945	-0.033
Aug	0.009	0.917	0.064
Sep	0.024	0.675	0.144
Oct	0.106	0.156	0.965
Nov	0.058	0.437	0.772
Dec	0.188	0.024*	3.367

$\alpha^* = 0.05, \alpha^{**} = 0.01$

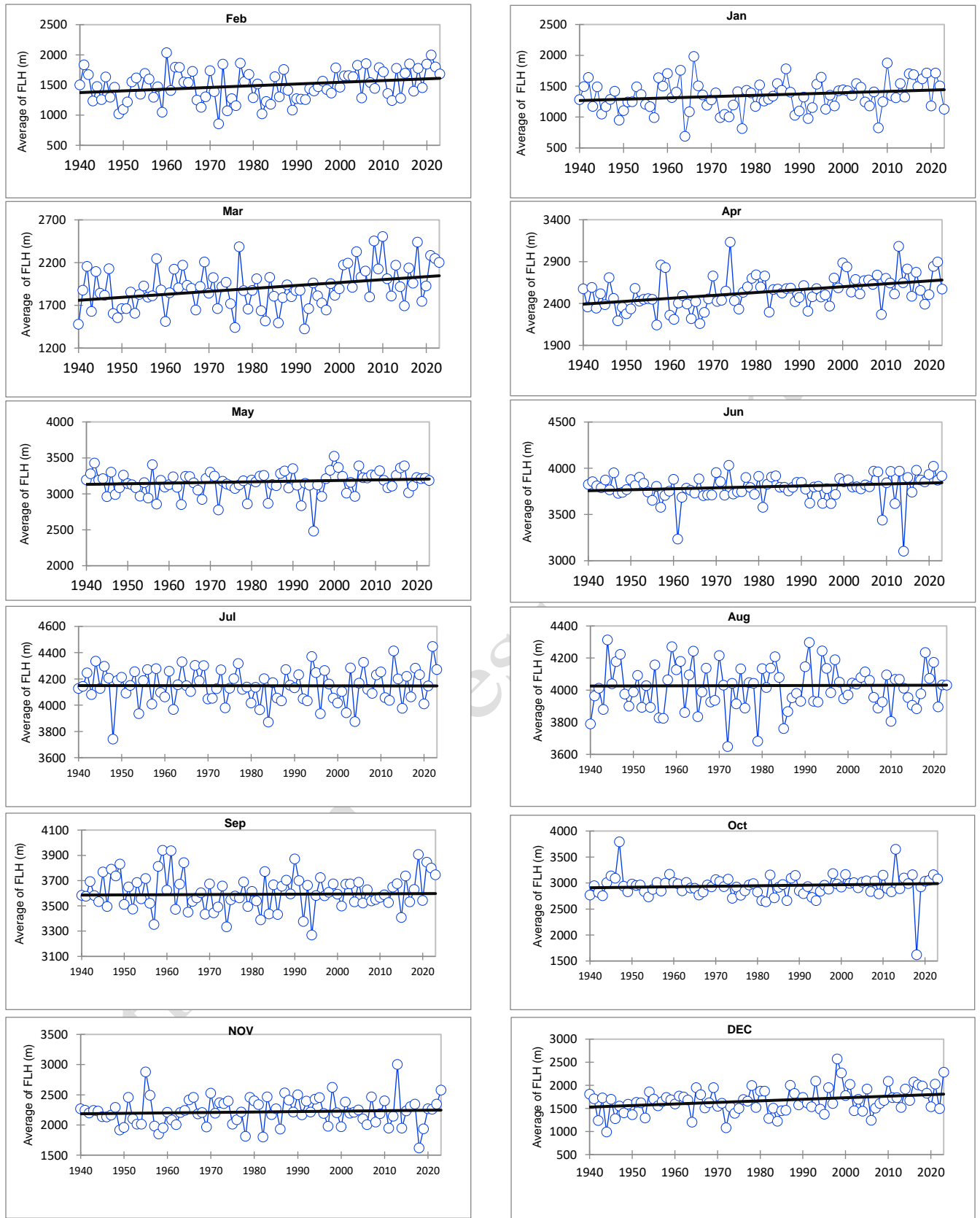


Figure 3. Mann-Kendall Trend and Sen's slope Graphs of Monthly FLH (1940-2023)

3.2. Seasonal trend analysis

The analysis results of the seasonal freezing level (Table 3 and Figure 4) show a significant increase in the winter, spring and, autumn seasons. The rate of increase in the height of the freezing level is higher in winter than in other seasons. This can justify the decreasing trend of snowfall in the region. Although the trend of changes in the height of the freezing level in summer shows a tendency to increase, but it is not significant. **These findings are consistent with studies in other regions. For example, the increasing trend of FLH in China is closely related to tropospheric warming and shows clear regional and seasonal variations (Guo et al., 2021). With a more pronounced increase in northern and western China during autumn and winter, it was found that FLH in the tropical atmosphere has increased in most regions, especially in the outer tropics, with an increase in surface and upper air temperatures of 0.1 °C per decade over the past 50 years in the tropical Andes (Bradley et al., 2009).**

Table 3. Seasonal Mann-Kendall Trend and Sen's slope of FLH (1940-2023)

Months	Kendall's tau	p-value	Sen's slope
Winter	0.239	< 0.0001**	2.698
Spring	0.241	0.001**	1.699
Summer	0.022	0.772	0.136
Autumun	0.172	0.008**	1.516

$\alpha^* = 0.05, \alpha^{**} = 0.01$

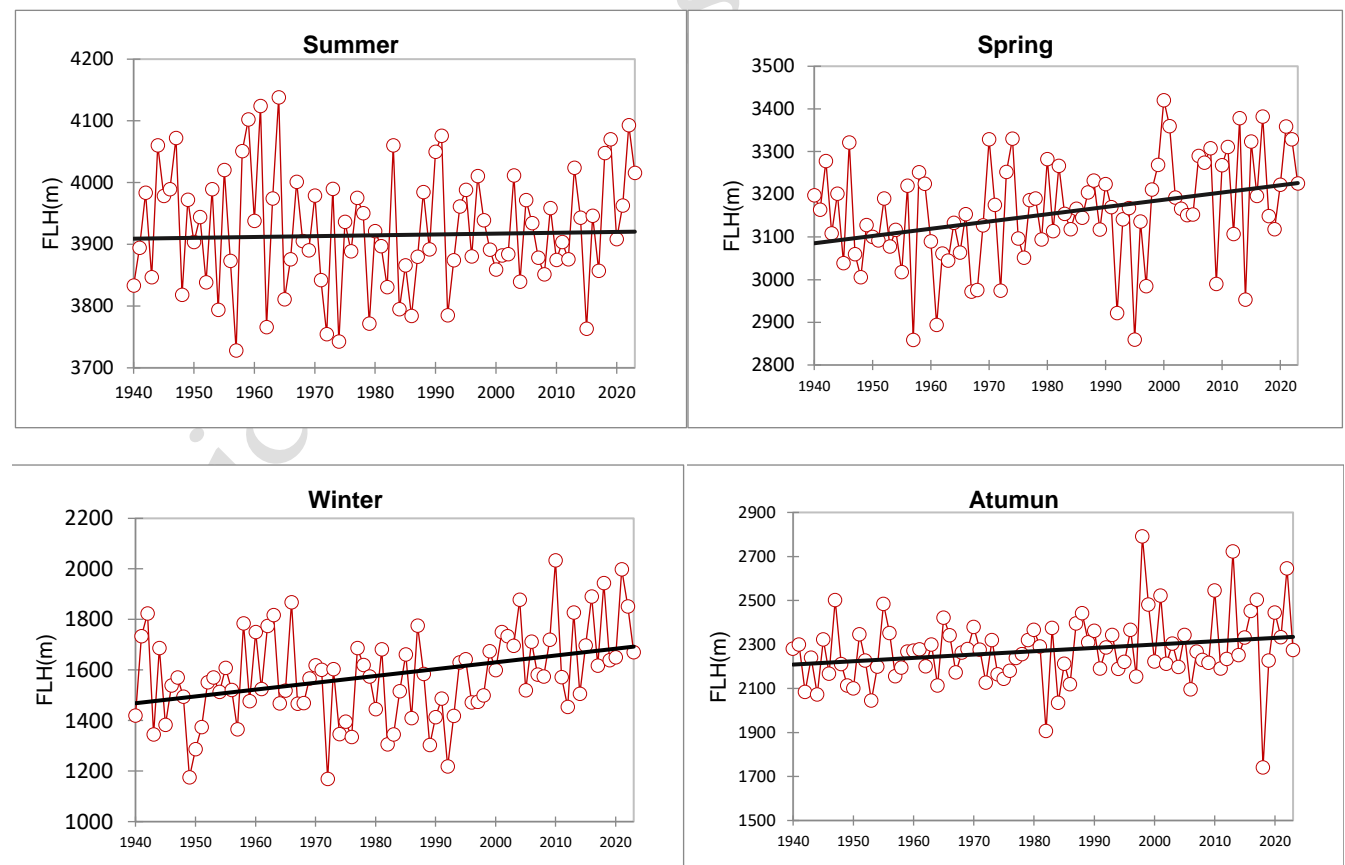


Figure 4. Mann-Kendall Trend and Sen's slope Graphs of Seasonal FLH (1940-2023)

3.3. Annual trend analysis

The annual trend analysis shows that the height of the FLH has an increasing trend at the alpha level of 0.01 (Table 4 and Figure 5). On average, the increase in the height of the FLH is 12.2 meters per decade. The analysis results of monthly, seasonal, and annual trends prove the increase in FLH as one of the consequences of global warming and climate change in the study area.

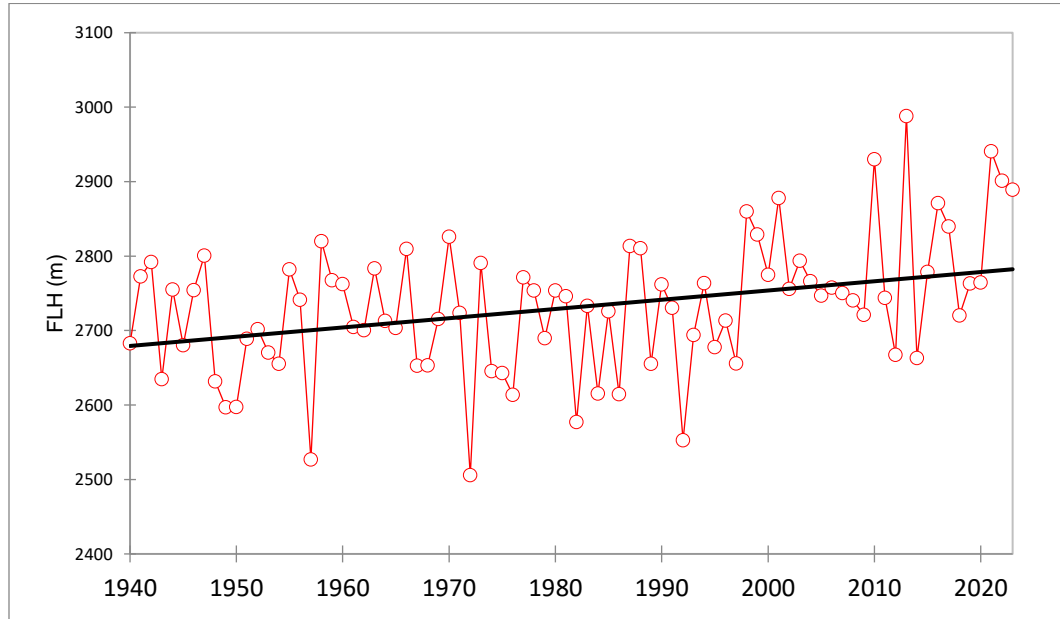


Figure 5. Mann-Kendall Trend and Sen's slope Graphs of Annual Average FLH (1940-2023)

Table 4. Annual Average Mann-Kendall Trend and Sen's slope of FLH (1940-2023)

Series	Kendall's tau	p-value	Sen's slope
Annual	0.239	0.001**	1.241

$\alpha^* = 0.05, \alpha^{**} = 0.01$

3.4. Spatial analysis

Due to the similarity of the monthly, seasonal, and annual distribution patterns of the freezing level height maps, only the spatial analysis results on a seasonal and yearly scale are presented in this section. The results of examining the spatial changes show that the height of the freezing level has an inverse relationship with the geographic latitude, and as the latitude decreases (towards southern regions of Iran), the height of the freezing level increases. This relationship is stronger in winter and autumn, and as we get closer to the warm season, this relationship becomes weaker (Figure 6).

The correlation coefficient of the changes of FLH with latitude is significant at the alpha level of 0.05 and shows that the region's latitude affects FLH. Based on the analysis of the maps, the lowest value of FLH in the entire period is observed on AIAM KOUH (52° E , 36°N) in the central Alborz in the north of Iran, and the highest freezing level is observed in the southeastern regions of the country and around Chabahar (61.5°E , 25.25°N) port (Figure 6).

The spatial distribution of the freezing level height on a seasonal scale shows that the slope of the freezing surface increases from north to south and west to east (Figures 7 and 8).

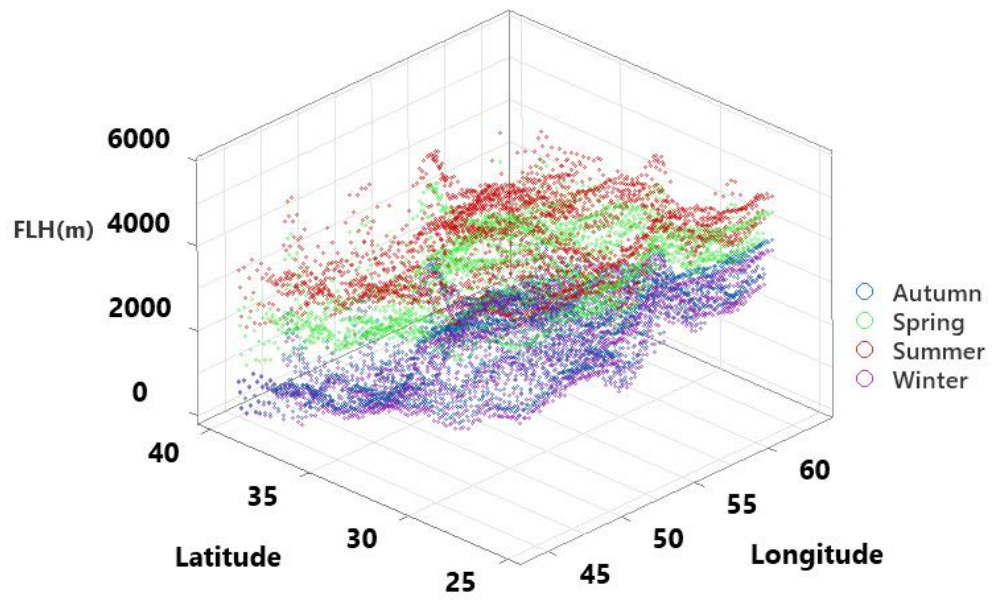


Figure 6. 3D spatial distribution of seasonal FLH in Iran (1940-2023)

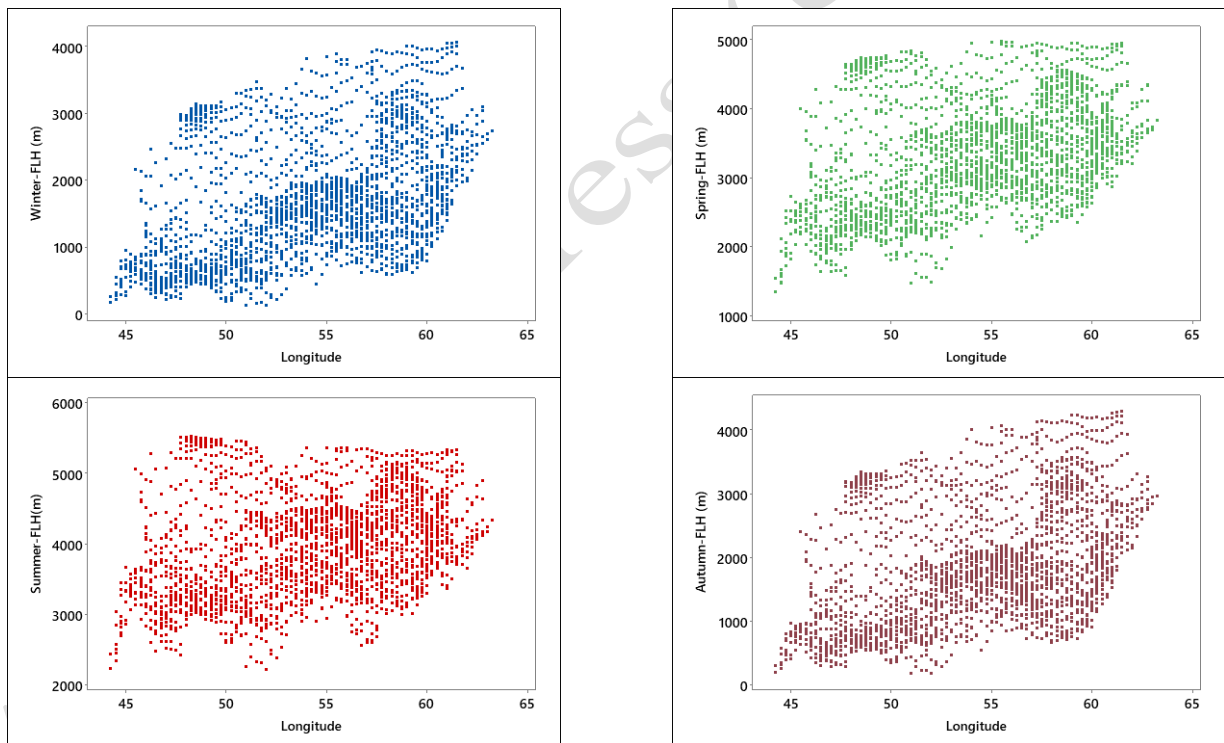


Figure 7. Seasonal spatial distribution of FLH (1940-2023) with longitude

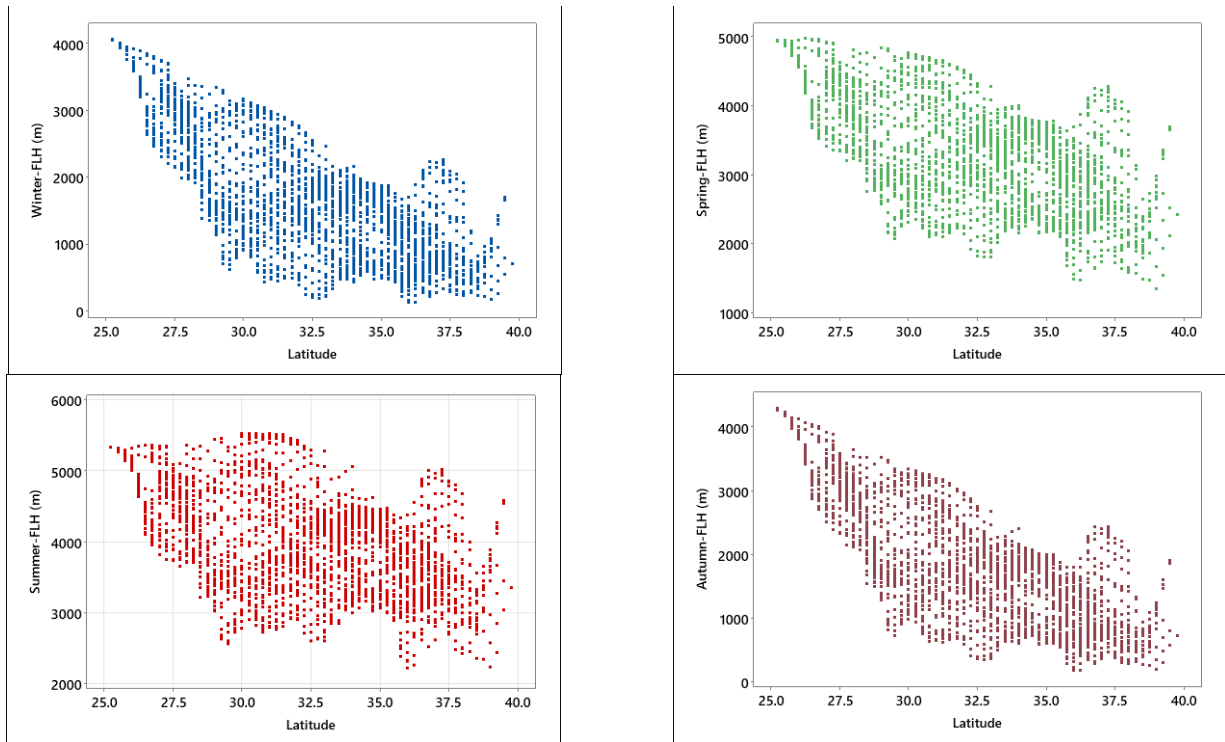


Figure 8. Seasonal spatial distribution of FLH (1940-2023) with latitude

The relationship between the height of the freezing level and the geographic length is direct. As we move from west to east (increasing longitude), FLH increases (Figure 9). It is clear that the western half of the country is mountainous, which has caused the temperature to decrease, and as a result, the height of the freezing level is low. The eastern half of the country has a lower altitude, as well as weak vegetation and bare soil causing an increase in surface temperature and naturally the freezing level rises. **This can reveal the relationship between freezing level height and surface temperature. Therefore, the relationship between FLH and near-surface temperature is consistent with the results of previous studies (Diaz and Graham, 1996; Harris et al., 2000).**

The value of the correlation coefficient of the height of the freezing level with latitude and longitude shows that the highest correlation value is observed in the autumn season and the lowest in the summer season (Table 4).

Table 4. The value of correlation coefficient FLH with latitude and longitude

Season	<i>X</i>	<i>Y</i>	<i>P-value</i>
Autumn	0.4708	-0.7514	0.0000
Spring	0.4501	-0.5876	0.0000
Summer	0.3221	-0.4637	0.0000
Winter	0.4828	-0.7415	0.0000
Annual	0.4445	-0.6593	0.0000

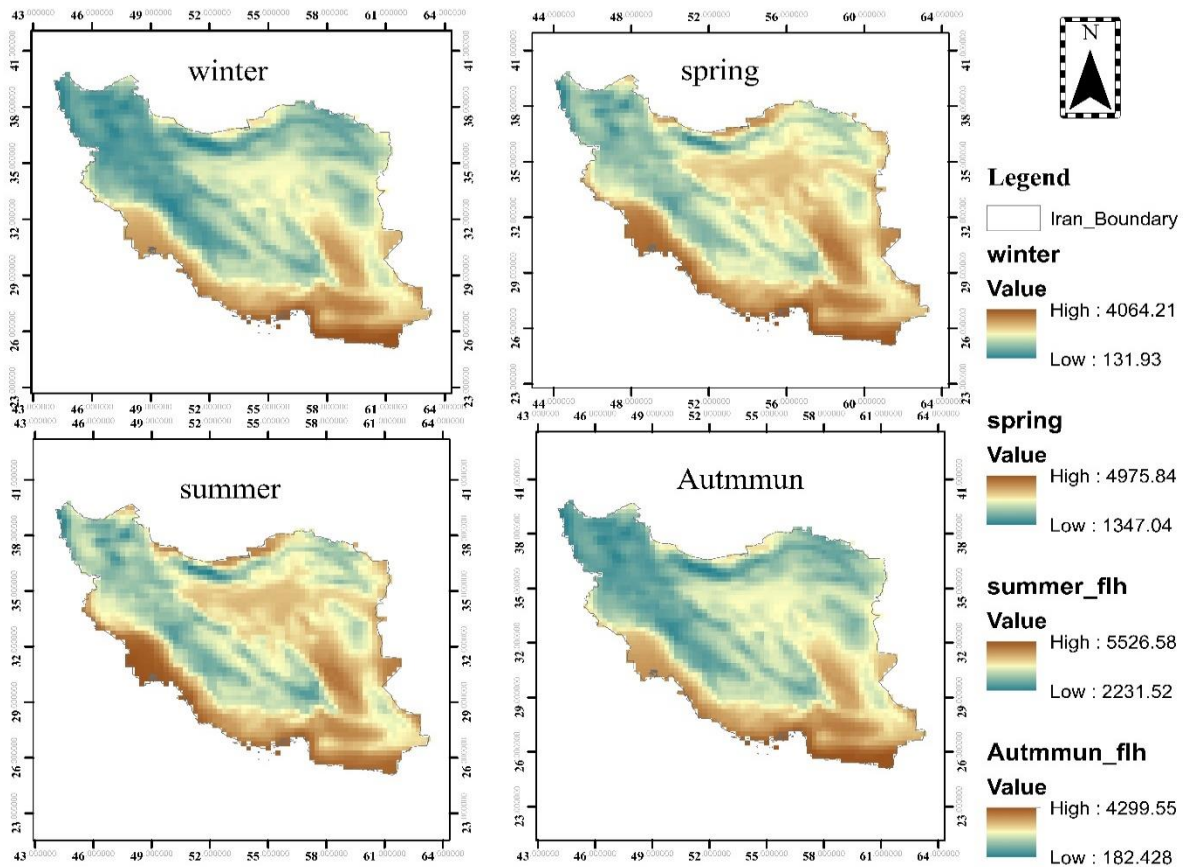


Figure 9. Raster map of seasonal FLH in Iran (1940-2023)

The annual pattern of spatial distribution of freezing level height is similar to the seasonal one (Figure 10). The effect of longitude and latitude is significantly visible in the annual spatial pattern (Figure 11 and Table 4). In the annual pattern, the Alam-Kuh areas have the lowest average height of the freezing level, and Chabahar (4347.5 meters) in southeastern Iran has the highest average freezing level height (Figure 12).

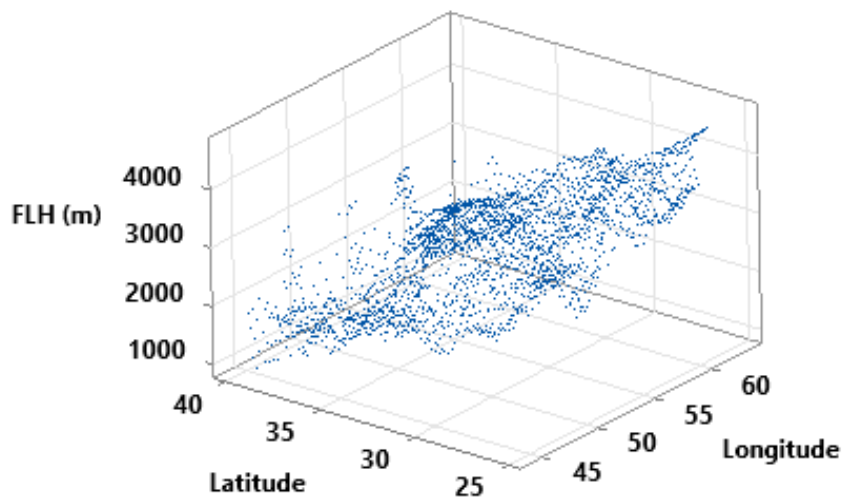


Figure 10. The pattern of spatial distribution of Annual FLH (1940-2023)

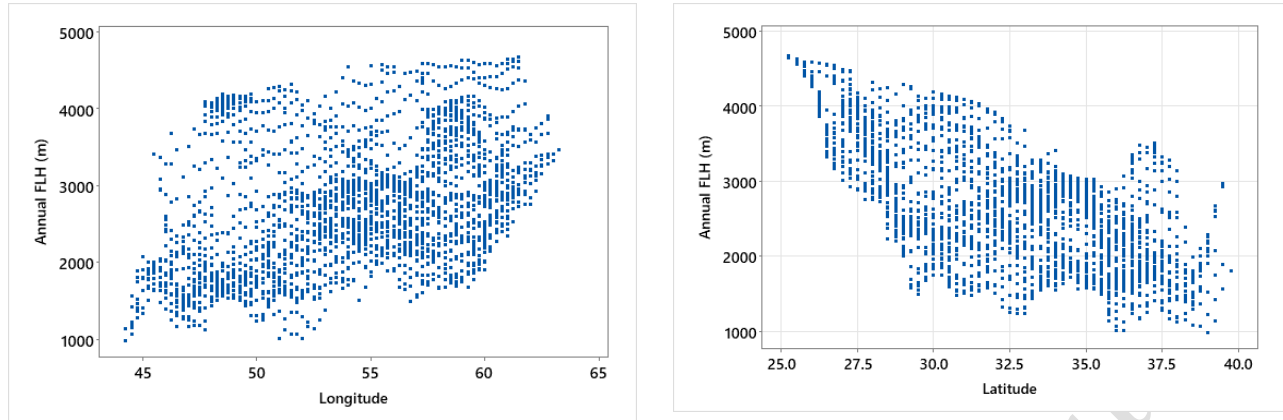


Figure 11. Spatial Distribution of Annual FLH (1940-2023) with latitude and longitude.

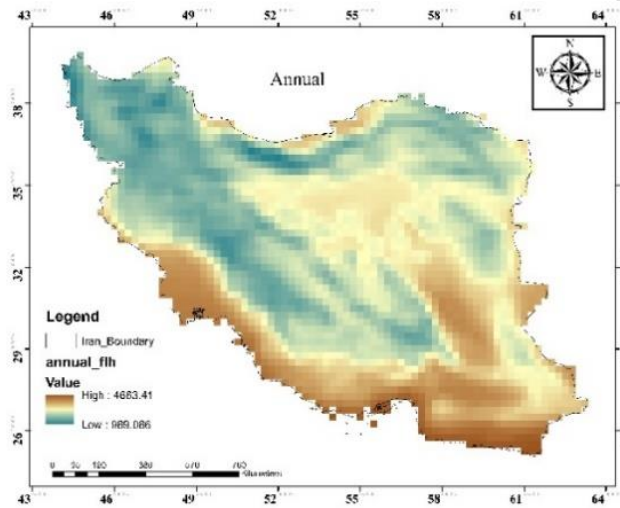


Figure 12. Annual Pattern of FLH (1940-2023)

3.5. Comparison of radiosonde data and reanalysis data

The values of FLH are data of upper atmosphere levels and cannot be measured through the network of ground-level stations. On the other hand, the very few number of upper atmosphere stations in Iran, the inadequacy and continuity of data, and the location of these stations within urban environments that act like heat islands and cannot reflect the natural conditions of freezing level height, the analysis of the trend of changes in FLH using statistical methods cannot be followed, therefore, only a case-by-case comparison of the ERA5 reanalysis data with the data of the country's stations on a specific day at a few upper atmosphere stations has been considered (Table 5). The results show that the data are largely close to each other, especially in January and February.

Table 5. Comparison of FLH radiosonde data and reanalysis data

ECMWF(m)	Radiosonde(m)	Station	hour	Date
1965	2225	Mehrabad	12	1/1/2020
1673	1872	Tabriz	12	1/1/2020
3712	3943	Zahedan	00	15/3/2020
2873	3050	Kermanshah	00	15/3/2017
2606	2850	Esfahan	00	15/3/2017

2401	2539	Ahwaz	00	1/1/2016
1412	1501	Esfahan	00	15/10/2021

The FLH at observation stations is slightly higher, which could be due to two factors: First: environmental effects (higher urban heat) on radiosonde. Second: Reanalysis data is the average of a range that can vary depending on spatial resolution, while radiosonde data are recorded as points. Also, when the wind blows, the radiosonde's ascent path is not vertical and shows different temperature gradients at different altitudes; especially when encountering an inversion layer. In this case, comparing radiosonde data with reanalysis data is difficult. Khansalari (2020) also emphasizes that the local and point-by-point study of the freezing level height is mostly the result of the passage of weather systems and the synoptic conditions of the month or season and cannot reflect the consequences of climate change.

4. Conclusion

With global warming and climate change in recent years, the study of changes in the freezing level height has attracted the attention of many atmospheric scientists. Changes in the critical zero-degree Celsius threshold will lead to changes in atmospheric circulation patterns, precipitation regimes, and the intensity of weather events.

Investigations of monthly changes in freezing level height show that the lowest FLH value occurs during January and fluctuates from ground level (zero) to the maximum height of 4347.5 meters. The maximum height of the freezing level reaches 5894.1 meters in August in the southeast of Iran (Chabahar). The highest coefficient of variation in the freezing level height in January ($cv=12.9$) (due to the passage of cold weather systems over the region), and the lowest in July ($cv=3.6$) (due to the establishment of subtropical high pressure and the stability of the atmosphere in the summer months) has been observed. The average height of the freezing level reaches its lowest level in winter (1576.7) and its highest level in summer, i.e. 3924.7 meters. The maximum range of changes in the average height of the FLH is 1049.9 meters which is observed in the autumn season. The mean annual FLH is 2733.7 meters with a standard deviation of 139.6. The average annual fluctuation of FLH is 721.6 meters (the Average annual minimum FLH is 2374 meters and the Average maximum annual FLH is 3095.6 meters).

In general, the trend of temporal changes of FLH on a monthly scale shows a significant increase in the alpha level of 0.5 from December to April (the cold period of the year). The highest increasing slope is observed in April. Seasonal changes in freezing level are somewhat similar to monthly changes and follow the same trend. Seasonal variations in FLH, such as monthly, show an increasing trend in winter, spring, and autumn. The highest increasing slope was observed in the winter season. The freezing level height in the summer season does not show a significant trend. In the annual scale, the changes in the freezing level height show a significant increasing trend at the alpha level of 0.01.

The spatial changes in the freezing level height show a significant relationship with the longitude and latitude in Iran. As the latitude increases, the height of the glacier surface decreases. On the other hand, with the increase in longitude, the height of FLH also increases (This issue can be caused by the weakness of vegetation and the increase in soil surface temperature in the lowland areas of the south and especially the southeast of Iran compared to the mountainous areas of the west and north of the country). The degree and intensity of the relationship between the freezing level height and the geographical location is greater in the winter months.

Given the decrease in snow cover and the increase in heavy precipitation in Iran, long-term assessment of changes in freezing level elevation can improve the prediction of these variables, so that water resources can be managed more optimally.

References

Bradley, R.S., Keiming, F.T., Diaz, H.F., & Hardy, D.R. (2009) Recent changes in freezing level heights in the tropics with implications for the deglaciation of high mountain regions. *Geophysical Research Letters*, 36, L17701. <https://doi.org/10.1029/2009GL037712>.

- Chen, Z., Chen, Y., & Li, W. (2012) Response of runoff to change of atmospheric 0C level height in summer in arid region of Northwest China. *Science China Earth Sciences*, 55(9), 1533– 1544. <https://doi.org/10.1007/s11430-012-4472-6>.
- Dessens, J. (1986) Hail in southwestern France. I: Hailfall characteristics and hailstorm environment. *Journal of Climatology & Applied Meteorology*, 25, 35–47. [https://doi.org/10.1175/1520-0450\(1986\)0252.0.CO;2](https://doi.org/10.1175/1520-0450(1986)0252.0.CO;2).
- Diaz, H.F., & Graham, N.E. (1996) Recent changes in tropical freezing heights and the role of sea surface temperature. *Nature*, 383, 152–155. <https://doi.org/10.1038/383152a0>.
- Diaz, H.F., Bradley, R.S., & Ning, L. (2014) Climatic changes in mountain regions of the American cordillera and the tropics: historical changes and future outlook. *Arctic Antarctic & Alpine Research*, 46(4), 735–743.
- Diaz, H.F., Eischeid, J.K., Duncan, C., & Bradley, R.S. (2003) Variability of freezing levels, melting season indicators, and snow cover for selected high-elevation and continental regions in the last 50 years. *Climatic Change*, 59, 33–52. <https://doi.org/10.1023/A:1024460010140>
- Dong, Z., Qin, D., Ren, J., Li, K., & Li, Z. (2012) Variations in the equilibrium line altitude of Urumqi Glacier No.1, Tianshan Mountains, over the past 50 years. *Chinese Science Bulletin*, (57), 4776–4783. <https://doi.org/10.1007/s11434-012-5524-1>.
- Gaffen, D.J., Santer, B.D., Boyle, J.S., Christy, J.R., Graham, N.E., & Ross, R.J. (2000) Multidecadal changes in the vertical temperature structure of the tropical troposphere. *Science*, 287, 1242–1245. <https://doi.org/10.1126/science.287.5456.1242>.
- Guo, Y., Wang, G., & Chao, Q. (2021) Climatological analysis of freezing level height over China and its implications using homogenized in-situ data. *International Journal of Climatology*.1-18. DOI: 10.1002/joc.7260
- Hamed, K.H. (2009) Exact distribution of the Mann–Kendall trend test statistic for persistent data, *Journal of Hydrology*, 365(1-2): 86–94. <https://doi.org/10.1016/j.jhydrol.2008.11.024>.
- Hamed, K.H., Rao, A.R. (1998) A modified Mann-Kendall Trend test for autocorrelated data, *Journal of Hydrology*, 204(1-4): 182–196. [https://doi.org/10.1016/S0022-1694\(97\)00125-X](https://doi.org/10.1016/S0022-1694(97)00125-X).
- Harris, G., Bowman, K., & Shin, D.B. (2000) Comparison of freezing-level altitudes from the NCEP reanalysis with TRMM precipitation radar bright band data. *Journal of Climate*, 13, 4137–4148. [https://doi.org/10.1175/1520-0442\(2000\)0132.0.CO;2](https://doi.org/10.1175/1520-0442(2000)0132.0.CO;2).
- Huang, X., Wang, S., Wang, J., Li, Y., Feng, J., & Zhang, K. (2013) Spatio-temporal changes in free-air freezing level heights in Northwest China. 1960-2012. *Quaternary International*, 313 (314), 130–136. <https://doi.org/10.1016/j.quaint.2013.07.200>.
- Khansalari, S. (2020) climate change in the height of the freezing line and its synoptic analysis at the airports of Mehrabad, Mashhad and Kermanshah. *Journal of Meteorology and Atmospheric Sciences*, Vol 3, 201-223.
- Khorshiddoust.A, Rasouli.A, Zanganeh.S.(2018) Modeling and trending of temperature and precipitation extreme indices in Lake Urmia basin. *Natural Hazards Journal*, Vol 7, 175-194.
- Lornezhad, E., Ebrahimi, H., Rabieifar, H.R. (2023) Analysis of precipitation and drought trends by a modified Mann–Kendall method: a case study of Lorestan province, Iran, *Water Supply*, 23 (4): 1557–1570. <https://doi.org/10.2166/ws.2023.068>
- Muia V. K., Opere A. O., Ndunda E., Amwata D. A. (2024) Rainfall and Temperature Trend Analysis using Mann-Kendall and Sen's Slope Estimator Test in Makueni County, Kenya. *J. Mater. Environ. Sci.*, 2024, Vol 15, Issue 3, Page 349-367
- Pepin, N., Bradley, R.S., Diaz, H.F., Baraer, M., Caceres, E. B., Forsythe, N., Fowler, H., Greenwood, G., Hashmi, M. Z., Liu, X. D., Miller, J. R., Ning, L., Ohmura, A., Palazzi, E., Rangwala, I., Schonert, W., Severskiy, I., Shahgedanova, M., Wang, M. B., Williamson, S.N., & Yang, D.Q. (2015) Elevation dependent warming in mountain regions of the world. *Nature Climate Change*, 5, 424–430. <http://doi.org/10.1038/NCLIMATE2563>
- Seidel, D.J., & Free, M. (2003) Comparison of lower-tropospheric temperature climatologies and trends at low and high elevation radiosonde sites. *Climatic Change*, 59, 53–74. <https://doi.org/10.1023/A:1024459610680>.

- Shi, P., Ma, X., Chen, X., Qu, S., Zhang, Z. 2013. Analysis of variation trends in precipitation in an upstream catchment of the Huai River. *Mathematical Problems in Engineering*, Article ID: 929383.
- Wang, S., Zhang, M., Pepin, N.C., Li, Z., Sun, M., Huang, X., & Wang, Q. (2014) Recent changes in freezing level heights in high Asia and their impact on glacier changes. *Journal of Geophysical Research Atmospheres*, 119, 1753–1765. [https://doi.org/ 10.1002/2013JD020490](https://doi.org/10.1002/2013JD020490).
- Zhang, G., Li, Z., Wang, W., & Wang, W. (2014a) Rapid decrease of observed mass balance in the Urumqi glacier no. 1, Tianshan Mountains, Central Asia. *Quaternary International*, 349(28), 135–141. <https://doi.org/10.1016/j.quaint.2013.08.035>.
- Zhang, M., Dong, L., Wang, S., Zhao, A., Qiang, F., Sun, M., & Wang, Q. (2014b) Increasing free-air 0C isotherm height in Southwest China from 1960 to 2010. *Journal of Geographical Sciences*, 24(5), 833–844. <https://doi.org/10.1007/s11442-014-1123-1>.
- Zhang, Y., & Guo, Y. (2011) Variability of atmospheric freezing-level height and its impact on the cryosphere in China. *Annals of Glaciology*, 52, 81–88. <https://doi.org/10.3189/172756411797252095>.

Article in Press (Unedited)